1521-0103/351/2/308–316$25.00
THE JOURNAL OF PHARMACOLOGY AND EXPERIMENTAL THERAPEUTICS

http://dx.doi.org/10.1124/jpet.114.215152
J Pharmacol Exp Ther 351:308–316, November 2014

Prevention of Bleomycin-Induced Lung Inflammation and Fibrosis in Mice by Naproxen and JNJ7777120 Treatment

Arianna Carolina Rosa, Alessandro Pini, Laura Lucarini, Cecilia Lanzi, Eleonora Veglia, Robin L. Thurmond, Holger Stark, and Emanuela Masini

Departments of Drug Science and Technology, University of Turin, Turin, Italy (A.C.R., E.V.); Department of Neuroscience, Psychiatry, and Drug Research, Section of Pharmacology (L.L., C.L., E.M.), and Experimental and Clinical Medicine (A.P.), University of Florence, Florence, Italy; Janssen Research & Development, L.L.C., San Diego, California (R.L.T.); and Heinrich-Heine Düsseldorf University, Institute of Medicinal Chemistry, Düsseldorf, Germany (H.S.)

Received April 23, 2014; accepted August 28, 2014

ABSTRACT

Pulmonary fibrosis, a progressive and lethal lung disease characterized by inflammation and accumulation of extracellular matrix components, is a major therapeutic challenge for which new therapeutic strategies are warranted. Cyclooxygenase (COX) inhibitors have been previously utilized to reduce inflammation. Histamine H_4 receptor (H_4R), largely expressed in hematopoietic cells, has been identified as a novel target for inflammatory and immune disorders. The aim of this study was to evaluate the effect of JNJ7777120 (1-[(5-chloro-1*H*-indol-2-yl)carbonyl]-4-methylpiperazine), a selective H_4R antagonist, and naproxen, a well known nonsteroidal anti-inflammatory drug, and their combination in a murine model of bleomycin-induced fibrosis. Bleomycin (0.05 IU) was instilled intratracheally to C57BL/6 mice, which were then treated by micro-osmotic pump with vehicle, JNJ7777120 (40 mg/kg b.wt.), naproxen (21 mg/kg b.wt.), or a combination of both. Airway resistance to inflation, an index of lung stiffness, was assessed, and lung specimens were processed for inflammation, oxidative stress, and fibrosis markers. Both drugs alone were able to reduce the airway resistance to inflation induced by bleomycin and the inflammatory response by decreasing COX-2 and myeloperoxidase expression and activity and thiobarbituric acid–reactive substance and 8-hydroxy-2′-deoxyguanosine production. Lung fibrosis was inhibited, as demonstrated by the reduction of tissue levels of transforming growth factor-β, collagen deposition, relative goblet cell number, and smooth muscle layer thickness. Our results demonstrate that both JNJ7777120 and naproxen exert an anti-inflammatory and antifibrotic effect that is increased by their combination, which could be an effective therapeutic strategy in the treatment of pulmonary fibrosis.

Introduction

Pulmonary fibrosis is a disease causing considerable morbidity and mortality, and it is one of the major therapeutic challenges (Hauber and Blaukovitsch, 2010; Raghu et al., 2011).

The hallmark of pulmonary fibrosis is a pathophysiologic response of the lungs to chronic injury and inflammation that manifests as abnormal and excessive deposition of collagen and other extracellular matrix components. Accumulation of vascular exudates and inflammatory cells within the injured alveolar space leads to epithelial cell injury. These exudates enhance the proliferation of resident fibroblasts and their transdifferentiation into myofibroblasts (activated collagen-secreting fibroblasts), as well as the transformation of epithelial cells, a typical feature of all fibrotic diseases (Kisseleva and Brenner, 2008). The myofibroblasts, organized into agglomerations of cells known as fibroblastic foci, produce an excessive tissue matrix, especially collagen, and the fibrosis becomes established (du Bois, 2010). This results in progressive airway stiffening and thickening of the air-blood membrane, which makes breathing difficult and eventually leads to respiratory failure.

Compelling evidence suggests that inflammatory cells influence fibrosis by releasing profibrotic mediators (Stramer et al., 2007). However, there is no effective available therapy that can favorably influence the course of the disease (Hauber and Blaukovitsch, 2010; Raghu et al., 2011). The use of glucocorticoids or immunosuppressive medications has been the conventional pharmacologic approach, although current reviews suggest that there is no therapeutic benefit with these drugs in comparison with their significant side effects (Carter, 2011). In this context, nonsteroidal anti-inflammatory drugs (NSAIDs), inhibiting the biosynthesis of prostanoids, have been proposed as a possible therapy for pulmonary fibrosis. Naproxen, a well known classical NSAID, was found to be

This work was supported by COST Action BM0806 (to A.C.R., A.P., H.S., and E.M.); and by Ente Cassa di Risparmio di Firenze, Florence, Italy (to E.M.).

Some of the data in this study were presented previously: Pini A, Somma T, Formicola G, Thurmond RT, Bani D, and Masini E (2011) Prevention of bleomycin-induced pulmonary fibrosis by a selecetive histamine H_4R antagonist. *40th European Histamine Research Society Meeting*; 2011 May 11–14; Sochi, Russia; and published in abstract form in *Inflamm Res* **60**:S335.

dx.doi.org/10.1124/jpet.114.215152.

ABBREVIATIONS: COX, cyclooxygenase; H_4R, histamine H_4 receptor; IL-10, interleukin-10; JNJ7777120, 1-[(5-chloro-1*H*-indol-2-yl)carbonyl]-4-methylpiperazine; MDA, malonyldialdehyde; MPO, myeloperoxidase; NSAID, nonsteroidal anti-inflammatory drug; 8-OHdG, 8-hydroxy-2′-deoxyguanosine; PAO, pressure at the airway opening; PAS, periodic acid–Schiff; PGE_2, prostaglandin E_2; TBARS, thiobarbituric acid–reactive substance; TGF, transforming growth factor.

effective in reducing lung inflammation and preventing collagen accumulation in the model of bleomycin-induced lung fibrosis (Masini et al., 2005; Pini et al., 2012). However, the clinical relevance of NSAIDs is in question because of their ineffectiveness in improving pulmonary function or survival in patients with idiopathic pulmonary fibrosis (Davies et al., 2003; Richeldi et al., 2003). Our data suggest that prostaglandin biosynthesis inhibition could have favorable effects during the overt inflammatory phase of the disease but not when the fibrosis is already established (Pini et al., 2012). Therefore, options oriented toward new therapeutic targets and combined therapies that could override the limits of the existing anti-inflammatory drugs are urgently required. In particular, it could be possible to design combination-based approaches targeting events that are downstream in the disease cascade compared with those that are upstream, as fibroblast activation is crucial to disease progression (Sivakumar et al., 2012). In vitro studies have shown that histamine is able to stimulate foreskin fibroblast proliferation, collagen synthesis (Garbuzenko et al., 2002), and conjunctival fibroblast migration (Leonardi et al., 1999). The observation that the histamine H_4 receptor (H_4R) is present in the bronchial epithelial, smooth muscle, and microvascular endothelial cells of the lung (Gantner et al., 2002) suggests a possible involvement of this receptor in different airway diseases. More recently, Kohyama et al. (2010) demonstrated in human fetal lung fibroblasts that JNJ7777120 (1-[(5-chloro-1*H*-indol-2-yl)carbonyl]-4-methylpiperazine), a selective H_4R antagonist, prevents fibronectin-induced lung fibroblast migration, thus suggesting that H_4R could represent an attractive target for the development of new drugs for lung fibrosis treatment (Kohyama et al., 2010). In addition, H_4R antagonists were found to reduce collagen deposition and goblet cell hyperplasia in a model of allergic asthma (Cowden et al., 2010). The aim of the present study was to validate the hypothesis that a combination-based strategy with an H_4R antagonist and an NSAID could be effective in pulmonary fibrosis. For this purpose, we have evaluated the relative effect of the H_4R-selective antagonist JNJ7777120, naproxen, and their combination in the in vivo mouse model of bleomycin-induced lung fibrosis.

Materials and Methods

Animals. Fifty male C57BL/6 mice, ~2 months old and weighing 25–30 g, were used for the experiments. They were purchased from a commercial dealer (Harlan, Udine, Italy) and housed in a controlled environment for 3 days at 22°C with a 12-hour light/dark cycle before use. During the experimental period, the animals were maintained in the same conditions as reported above and provided with standard chow and water ad libitum. The experimental protocols were designed in compliance with the Italian and the European Community regulations on animal experimentation for scientific purposes (D.M. 116192; O.J. of E.C. L358/1 12/18/1986) and in agreement with good laboratory practice standards. The protocols were approved by the Ethical Committee of the University of Florence (Florence, Italy). Experiments were carried out at the Centre for Laboratory Animal Housing and Experimentation, University of Florence.

Surgery and Treatments. The mice were anesthetized with zolazepam/tiletamine (Zoletil; Virbac Srl, Milan, Italy; 50 μg/g in 100 μl of saline i.p.); 40 were treated with bleomycin (0.05 IU in 100 μl of saline) and the other 10 with 100 μl of saline (referred to as nonfibrotic negative controls), both delivered by intratracheal injection. The bleomycin-treated mice were randomly assessed to receive, by subcutaneously implanted micro-osmotic pump (ALZET Osmotic Pumps, Cupertino, CA), vehicle alone (referred to as fibrotic positive controls); JNJ7777120 (provided by Johnson & Johnson Pharmaceutical and Development, San Diego, CA; total dose of 40 mg/kg b.wt.); naproxen (total dose of 21 mg/kg b.wt.); or a combination of both for 15 days after surgery. The micro-osmotic pump allows the release of 0.11 μl/h of drug, for a daily dosage of 1.056 mg/kg for JNJ7777120 and 0.55 mg/kg for naproxen. The dose of JNJ7777120 administered with the micro-osmotic pump was selected as the lowest dose that exerted an effect in a subchronic model of asthma (Cowden et al., 2010). The naproxen dose (0.55 mg/kg per day) was selected according to our previous results obtained in the same animal model of fibrosis (Pini et al., 2012), in which 1 mg/kg showed the maximal effect; in the present study, we investigated the efficacy of the combination of the two compounds in order to reduce the toxicity of naproxen (ED_{50}, 3.7 mg/kg).

Functional Assay of Fibrosis. At day 14 after surgery, the mice were subjected to measurement of airway resistance to inflation, a functional parameter related to fibrosis-induced lung stiffness, using a constant-volume mechanical ventilation method (Masini et al., 2005). Briefly, upon anesthesia, the mice were operated on to insert a 22-gauge cannula (0.8-mm diameter, Venflon 2; BD, Brea, CA) into the trachea and then ventilated with a small-animal respirator (Ugo Basile, Bologna, Italy), adjusted to deliver a tidal volume of 0.8 ml at a rate of 20 strokes/min. Changes in lung resistance to inflation [pressure at the airway opening (PAO)] were registered by a high-sensitivity pressure transducer (P75 type 379; Hugo Saks Elektronik, March-Hugstetten, Germany) connected to a polygraph (Harvard Apparatus, Kent, UK) at the following settings: gain, 1; chart speed, 25 mm/s. Inflation pressure was measured for at least 3 minutes. In each mouse, PAO measurements (expressed as millimeters on the chart) were carried out on at least 40 consecutive tracings of respiratory strokes after breathing stabilization and then averaged.

Lung Tissue Sampling. After the functional assay, the animals were killed with a lethal dose of anesthetic drugs and the entire left lungs were excised and fixed by immersion in 4% formaldehyde in phosphate-buffered saline for histological analysis. The right lungs were weighed, quickly frozen, and stored at −80°C. When needed for the biochemical assays, these samples were thawed at 4°C; homogenized on ice in 50 mM Tris-HCl buffer containing 180 mM KCl and 10 mM EDTA, final pH 7.4; and then centrifuged at 10,000*g*, 4°C, for 30 minutes, unless otherwise reported. The supernatants and the pellets were collected and used for separate assays, as detailed below.

Histology and Computer-Aided Densitometry of Lung Collagen. Histological sections, 6 μm thick, were cut from paraffin-embedded lung samples and stained with H&E for routine observation and periodic acid–Schiff (PAS) or modified Azan method (Pini et al., 2010) for the evaluation of goblet cells and collagen deposition. Staining was performed in a single session to minimize the artifactual differences in collagen staining. For each mouse, 20 photomicrographs of peribronchial connective tissue were randomly taken using a digital camera connected to a light microscope with a 40× objective (test area of each micrograph, 38,700 μm^2). Measurements of optical density of the aniline blue–stained collagen fibers were carried out using the ImageJ 1.33 image analysis program (http://rsb.info.nih.gov/ij), upon appropriate threshold selection to exclude aerial air spaces and bronchial/alveolar epithelium, as previously described (Pini et al., 2010). For morphometry of smooth muscle layer thickness and bronchial goblet cell numbers, both key markers of airway remodeling, lung tissue sections were stained with H&E for smooth muscle layer thickness and with PAS for mucins. Digital photomicrographs of medium- and small-sized bronchi were randomly taken. Measurements of the thickness of the bronchial smooth muscle layer were carried out on the digitized images using the above-mentioned software. PAS-stained goblet cells and total bronchial epithelial cells were counted on bronchial cross-section profiles, and the percentage of goblet cells was calculated. For all these parameters, values are means ± S.E.M. of individual mice (20 images each) from the different experimental groups.

Determination of Transforming Growth Factor-β Levels. The levels of transforming growth factor (TGF)-β, the major profibrotic cytokine involved in fibroblast activation (Wynn, 2008), were measured on aliquots (100 μl) of lung homogenate supernatants using the Flow Cytomix assay (Bender MedSystems GmbH, Vienna, Austria), following the protocol provided by the manufacturer. Briefly, a suspension of anti-TGF-β–coated beads was incubated with the samples (and a TGF-β standard curve) and then with biotin-conjugated secondary antibodies and streptavidin-phycoerythrin. Fluorescence was read with a cytofluorimeter (Epics XL; Beckman Coulter, Milan, Italy). Values are expressed as picograms per milligram of protein, the latter determined with the Bradford method (Bradford, 1976) over an albumin standard curve.

Determination of Myeloperoxidase Activity. This tissue indicator of leukocyte recruitment was determined as described by the literature (Mullane et al., 1985). Briefly, frozen lung tissue samples of about 50–70 mg were homogenized in a solution containing 0.5% hexadodecyl trimethyl ammonium bromide dissolved in 10 mM potassium phosphate buffer, pH 7, and then centrifuged for 30 minutes at 20,000*g* at 4°C. An aliquot of the supernatant was then allowed to react with a solution of tetramethylbenzidine (1.6 mM) and 0.1 mM H_2O_2. The rate of change in absorbance was measured spectrophotometrically at 650 nm. Myeloperoxidase (MPO) activity was defined as the quantity of enzyme degrading 1 μmol of peroxide per minute at 37°C and was expressed in milliunits per milligram of protein, determined with the Bradford method (Bradford, 1976) over an albumin standard curve.

Determination of Prostaglandin E_2 and Interleukin-10 Levels. The levels of prostaglandin E_2 (PGE_2), the major cyclooxygenase product generated by activated inflammatory cells, and the levels of interleukin-10 (IL-10), a well known anti-inflammatory cytokine, were measured on aliquots (100 μl) of lung homogenate supernatants using commercial Biotrak enzyme-linked immunosorbent assay kits (Amersham Biosciences, Little Chalfont, Buckinghamshire, UK), following the protocol provided by the manufacturer. The values are expressed as nanograms per milligram of protein, the latter determined with the Bradford method (Bradford, 1976) over an albumin standard curve.

Determination of Oxidative Stress Parameters. Malonyldialdehyde (MDA) is an end product of peroxidation of cell membrane lipids caused by oxygen-derived free radicals; it is considered a reliable marker of inflammatory tissue damage. It was determined as thiobarbituric acid–reactive substance (TBARS) levels, as described previously (Ohkawa et al., 1979). Lung tissue (~100 mg) was homogenized with 1 ml of 50 mM Tris-HCl buffer containing 180 mM KCl and 10 mM EDTA, final pH 7.4. 2-thiobarbituric acid [0.5 ml, 1% (w/v)] in 0.05 M NaOH and 0.5 ml of HCl [25% (w/v) in water] were added to 0.5 ml of sample. The mixture was placed in test tubes, sealed with screw caps, and heated in boiling water for 10 minutes. After cooling, the chromogen was extracted in 3 ml of 1-butanol and the organic phase was separated by centrifugation at 2000*g* for 10 minutes. The absorbance of the organic phase was read spectrophotometrically at 532-nm wavelength. The values are expressed as nanomoles of TBARS (MDA equivalents) per milligram of protein, using a standard curve of 1,1,3,3-tetramethoxypropane.

As an indicator of oxidative DNA damage, levels of 8-hydroxy-2′-deoxyguanosine (8-OHdG) were determined as previously described (Lodovici et al., 2000). Briefly, lung samples were homogenized in 1 ml of 10 mM phosphate-buffered saline, pH 7.4; sonicated on ice for 1 minute; added to 1 ml of 10 mM Tris-HCl buffer, pH 8, containing 10 mM EDTA, 10 mM NaCl, and 0.5% SDS; and incubated for 1 hour at 37°C with 20 μg/ml of RNase 1 (Sigma-Aldrich, St. Louis, MO) and overnight at 37°C under argon in the presence of 100 μg/ml of proteinase K (Sigma-Aldrich). The mixture was extracted with chloroform/isoamyl alcohol [10:2 (v/v)]. DNA was precipitated from the aqueous phase with 0.2 volumes of 10 mM ammonium acetate; solubilized in 200 μl of 20 mM acetate buffer, pH 5.3; and denatured at 90°C for 3 minutes. The extract was then supplemented with 10 IU of P1 nuclease (Sigma-Aldrich) in 10 μl of PBS and incubated for 1 hour at 37°C with 5 IU of alkaline phosphatase (Sigma-Aldrich) in 0.4 M phosphate buffer, pH 8.8. All of the procedures were performed in the dark under argon. The mixture was filtered by an Amicon Micropure-EZ filter (Millipore Corporation, Billerica, MA), and 50 μl of each sample was used for 8-OHdG determination using a Bioxytech enzyme immunoassay kit (Oxis, Portland, OR), following the instructions provided by the manufacturer. The values are expressed as nanograms of 8-OHdG per milligram of protein, the latter determined with the Bradford method (Bradford, 1976) over an albumin standard curve.

Determination of Smad3 Level Expression. Tissue samples were homogenized on ice and lysed as previously reported (Sassoli et al., 2012). Total protein extract (1 mg) was precleared by Protein G (Sigma-Aldrich) for 1 hour at 4°C. After centrifugation, the supernatants were collected and incubated overnight at 4°C with 4 μg of goat polyclonal anti-Smad4 antibody (Santa Cruz Biotechnology, Santa Cruz, CA). The immunocomplexes were recovered using Protein G, subjected to electrophoresis, blotted with rabbit polyclonal anti-Smad3 (1:1000 in Tris-buffered saline/Tween 20; Cell Signaling Technology, Danvers, MA), and then reprobed with anti-Smad4 antibody (1:1000 in Tris-buffered saline/Tween 20).

Statistical Analyses. For each assay, data were reported as mean values (± S.E.M) of individual average measures of the different animals per group. Significance of differences among the groups was assessed by one-way analysis of variance followed by Newman-Keuls post hoc test for multiple comparisons using GraphPad Prism 4.03 statistical software (GraphPad Software, Inc., La Jolla, CA).

Results

Functional Assay of Fibrosis. Intratracheal bleomycin caused a statistically significant increase in airway stiffness as judged by the significant elevation of PAO (Fig. 1) in the fibrotic positive controls compared with the nonfibrotic negative ones (+2.06 ± 0.25 mm; $P < 0.001$). Both naproxen and JNJ7777120 given alone caused a significant reduction of bleomycin-induced airway stiffness. The efficacy of JNJ7777120 seemed slightly higher than that of equimolar naproxen (−1.30 ± 0.21 and −1.07 ± 0.22 mm for JNJ7777120 and naproxen, respectively), although the differences did not

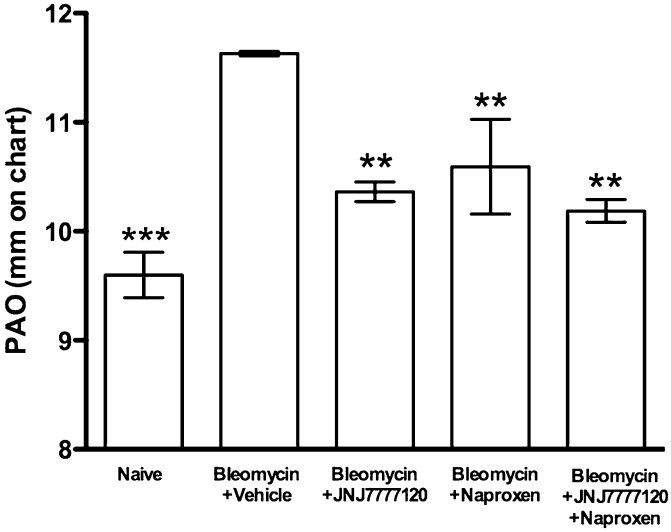

Fig. 1. Spirometric evaluation. Bar graph and statistical analysis of differences in PAO values (means ± S.E.M) between the different experimental groups (one-way analysis of variance; n = 10 animals per group). $^{**}P < 0.01$; $^{***}P < 0.001$ versus bleomycin + vehicle.

reach statistical significance. Similar results were obtained when the two drugs were coadministered.

Morphologic and Morphometric Analyses. Intratracheal bleomycin administration was found to cause lung inflammation and fibrosis. By computer-aided densitometry on Azan-stained sections (Fig. 2), which allows the determination of the optical density of collagen fibers, the lungs of the fibrotic positive controls demonstrated an increase in collagen fibers, which was significantly reduced by both JNJ7777120 and naproxen given alone ($P < 0.01$ and $P < 0.05$, respectively). When the two drugs were given together, a trend toward an increased effect was observed. The extent of the inflammatory infiltrate, which was composed mainly of macrophages, lymphocytes, and neutrophils, was reduced by all the treatments. We then evaluated bronchial remodeling by measuring the relative number of goblet cells (Fig. 3) and the thickness of the smooth muscle (Fig. 4), key histological parameters of inflammation-induced adverse bronchial remodeling (Bai and Knight, 2005). As expected, both these parameters were significantly increased after intratracheal bleomycin treatment (+10.09% ± 1.30%, $P < 0.001$ for goblet cell number; +27.38 ± 3.35 μm, $P < 0.001$ for thickness of the smooth muscle). JNJ7777120 and naproxen, both alone and in combination, were able to significantly reduce the percentage of PAS-positive goblet cells over total bronchial epithelial cells (−7.83% ± 1.21%, $P < 0.05$; and −5.74% ± 1.38%, $P < 0.05$, respectively), as well as the thickness of the airway smooth muscle layer (−22.40 ± 3.03 μm, $P < 0.01$; and −18.97 ± 3.50 μm, $P < 0.05$, respectively). Notably, the combination of the two drugs showed a statistically significant reduction of the fraction of goblet cells compared with treatment with naproxen alone (−4.46% ± 1.38%; $P < 0.05$).

Determination of Inflammation and Fibrosis Parameters. Assay of TGF-β (Fig. 5A), a major profibrotic cytokine, showed that this molecule was significantly increased in the fibrotic positive controls (+274.9 ± 13.68 pg/mg of protein;

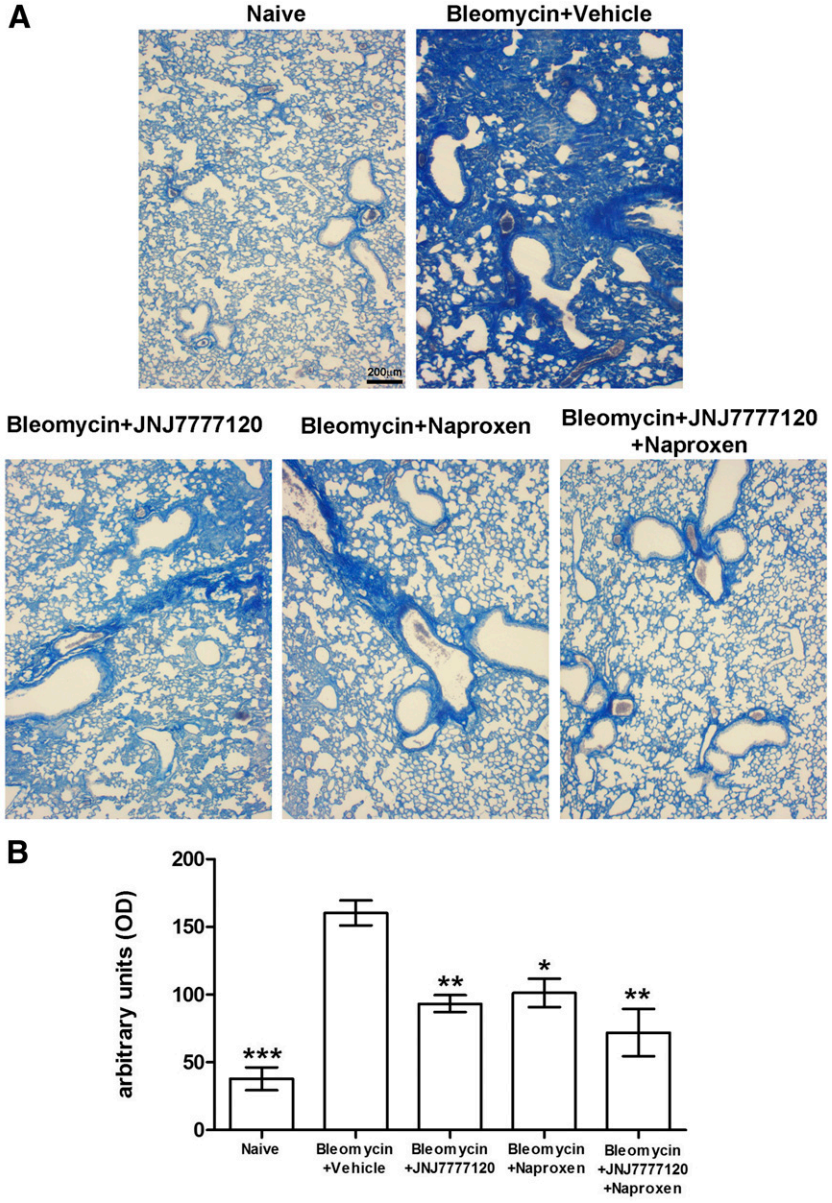

Fig. 2. Evaluation of lung fibrosis. (A) Representative micrographs of Azan-stained lung tissue sections from mice from the different experimental groups. Collagen fibers are stained deep blue. The lung from a fibrotic control treated with vehicle showed marked fibrosis in the peribronchial stroma, which was absent in the lung from a nonfibrotic negative control and reduced by both JNJ7777120 and naproxen either alone or in combination. (B) Bar graph showing the optical density (OD) (means ± S.E.M.) of Azan-stained collagen fibers of the different experimental groups (one-way analysis of variance; $n = 10$ mice per group). *$P < 0.05$; ** $P < 0.01$; ***$P < 0.001$ versus bleomycin + vehicle.

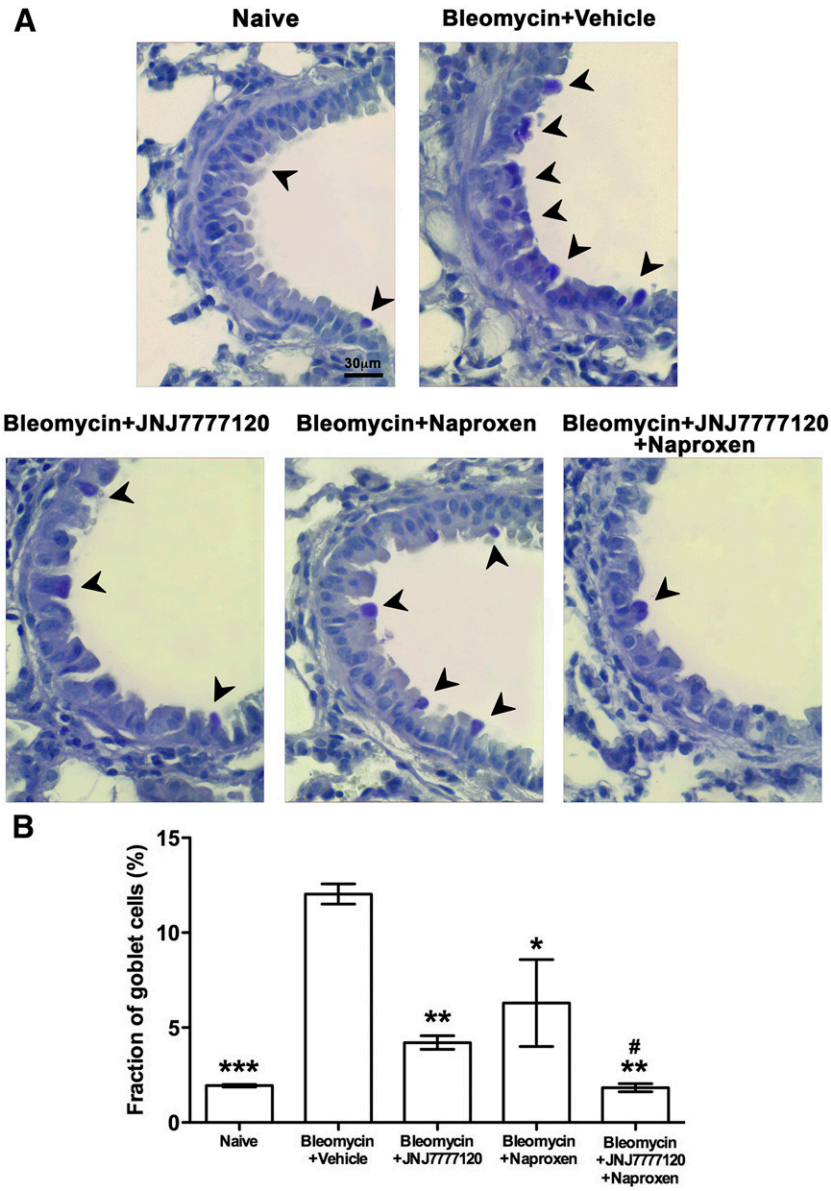

Fig. 3. Goblet cell hyperplasia. (A) Representative micrographs of PAS-stained sections. Arrows indicate the goblet cells. (B) Bar graph showing the fraction of goblet cells (% means ± S.E.M.) in the different experimental groups (one-way analysis of variance; $n = 10$ animals per group). $^{*}P < 0.05$; $^{**}P < 0.01$; $^{***}P < 0.001$ versus bleomycin + vehicle; $^{\#}P < 0.05$ versus bleomycin + naproxen.

$P < 0.001$). JNJ7777120 or naproxen treatment caused a statistically significant and comparable reduction of TGF-β (-116.2 ± 6.98 and -123.0 ± 6.84 pg/mg of protein, respectively; $P < 0.01$ for both). Notably, the coadministration of both drugs was more effective than JNJ7777120 or naproxen alone (-93.83 ± 6.68 pg/mg of protein versus JNJ7777120 and -87.12 ± 5.60 pg/mg of protein versus naproxen; $P < 0.01$). As the Smad3/4 complex is necessary for activation of TGF-β signaling (Chen et al., 2005), we investigated the effect of the pharmacologic treatment on the complex formation by Western blotting analysis performed on the immunoprecipitated Smad4 protein. As shown in Fig. 5B, just above the heavy chain of IgG we identified a 61-kDa protein band consistent with Smad4. Notably, when we blotted with the anti-Smad3 antibody, we observed a profound upregulation in the positive fibrotic controls, which was prevented by JNJ7777120 and naproxen given alone. Intriguingly, as shown for TGF-β levels, the coadministration of the two drugs was more effective.

Determination of MPO (Fig. 6A), an index of leukocyte accumulation into the inflamed lung tissue, showed that this parameter was significantly increased in the fibrotic positive controls compared with nonfibrotic negative ones. Administration of JNJ7777120 or naproxen caused a statistically significant reduction of MPO induced by bleomycin (-9.53 ± 0.28 and -9.39 ± 0.027 mU/mg of protein for JNJ7777120 and naproxen, respectively; $P < 0.001$). When the two drugs were coadministered, an increased effect was observed (-11.27 ± 0.34 mU/mg of protein; $P < 0.05$).

Determination of PGE_2 (Fig. 6B), the major cyclooxygenase product generated by activated inflammatory cells (fibroblasts included), showed that this mediator was markedly increased in the fibrotic positive controls compared with the nonfibrotic negative controls ($+52.08 \pm 2.69$ pg/mg of protein; $P < 0.001$). JNJ7777120 or naproxen given alone caused a statistically significant reduction of PGE_2 level, with naproxen, as expected, more effective than JNJ7777120 (-16.20 ± 2.36 pg/mg of protein for JNJ7777120 and -35.30 ± 2.36 pg/mg of protein

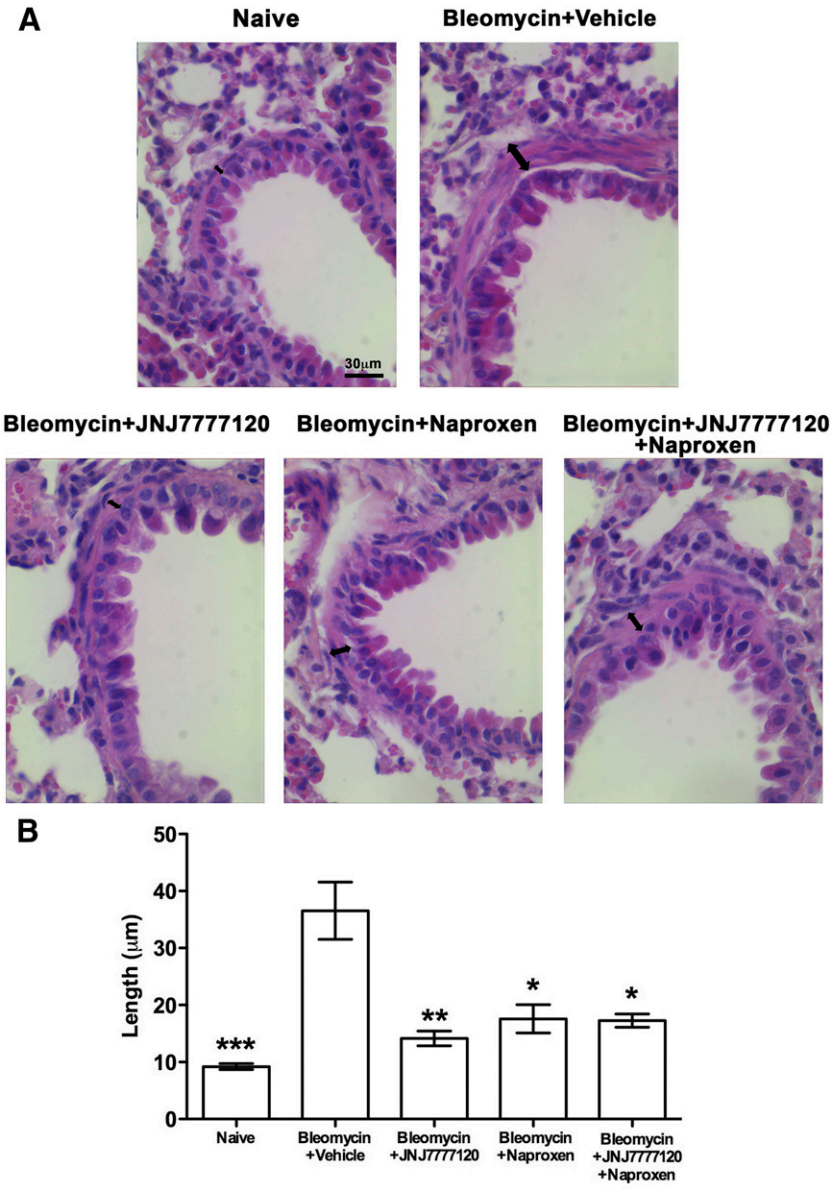

Fig. 4. Evaluation of the muscular remodeling. The smooth muscle thickness was assessed by computer-aided morphometry on H&E-stained lung sections. (A) Representative micrographs of the sections. The thickness of the smooth muscle layer is indicated by double arrows. (B) Bar graph showing the length of the muscular fiber (means ± S.E.M.) in the different experimental groups (one-way analysis of variance; $n = 10$ animals per group). *$P < 0.05$; **$P < 0.01$; ***$P < 0.001$ versus bleomycin + vehicle.

for naproxen; $P < 0.01$). However, the combination of the two drugs was more effective in reducing PGE_2 production in comparison with the single drugs (−28.26 ± 2.23 pg/mg of protein versus JNJ7777120, $P < 0.01$; −9.16 ± 2.23 pg/mg of protein versus naproxen, $P < 0.001$). To confirm the anti-inflammatory effects of the two studied drugs, we evaluated production of IL-10, a regulatory cytokine (Fig. 6C). As expected, bleomycin-treated animals showed a significant reduction in IL-10 levels (−17.05 ± 1.51 pg/mg of protein; $P < 0.001$), whereas the administration of both JNJ7777120 and naproxen alone and in combination caused a statistically significant increase in IL-10 levels ($P < 0.01$). When the two drugs were coadministered, a potentiated effect was observed.

Evaluation of Oxidative Stress Parameters. Measurement of TBARS (Fig. 7A), a reliable marker of oxidative tissue injury, being the end product of cell membrane lipid peroxidation by reactive oxygen species, and of 8-OHdG (Fig. 7B), an indicator of oxidative DNA damage, showed that they were markedly increased in fibrotic positive controls (+41.33 ± 11.15 nmol/mg of protein and +51.25 ± 2.77 ng/mg of protein, respectively; $P < 0.001$) compared with nonfibrotic negative controls; these parameters were significantly reduced by JNJ7777120 (−18.17 ± 5.66 nmol/mg of protein and −33.46 ± 2.65 ng/mg of protein, respectively; $P < 0.01$) or naproxen (−23.50 ± 7.32 nmol/mg protein and −33.48 ± 2.65 ng/mg of protein, respectively; $P < 0.01$). Notably, the combination of JNJ7777120 and naproxen was more effective in reducing MDA levels than JNJ7777120 (−14.08 ± 4.8 nmol/mg of protein; $P < 0.05$) or naproxen (−8.74 ± 2.98 nmol/mg of protein; $P < 0.01$) treatment alone. A slight but not significant effect was also observed in 8-OHdG production.

Discussion

The data presented in this work demonstrate the anti-inflammatory and antifibrotic properties of naproxen and JNJ7777120 in a mouse model of lung fibrosis. We selected the model of intratracheally-delivered bleomycin because it is

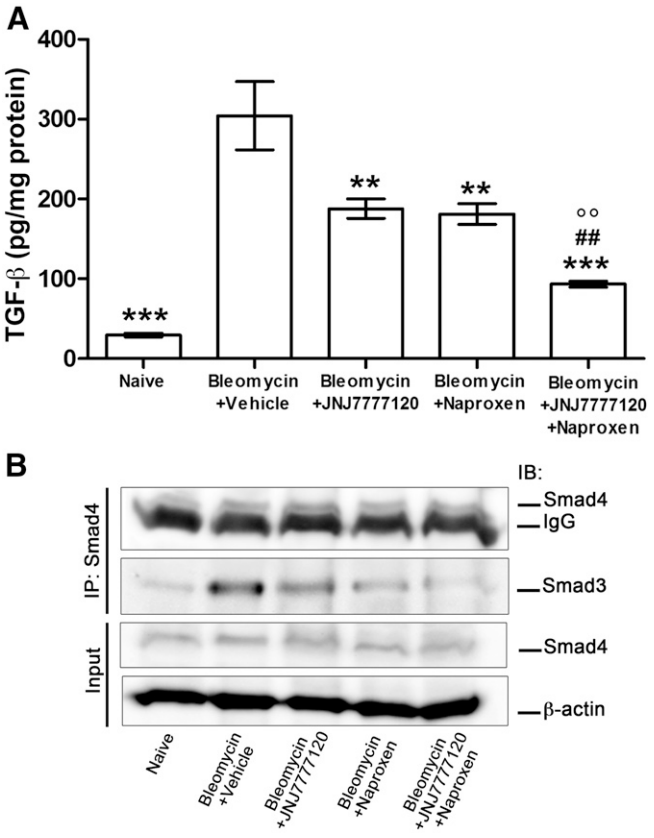

Fig. 5. Evaluation of fibrotic key mediators. (A) Bar graph showing the lung tissue levels of the profibrotic cytokine TGF-β (means ± S.E.M.) from mice from the different experimental groups (one-way analysis of variance; n = 10 animals per group). (B) Smad4 and Smad3 expression level in the noted experimental conditions, assayed by Western blotting analysis performed on the immunoprecipitated Smad4 protein. Note that the profound upregulation of Smad3 expression level in the positive fibrotic control was prevented by the treatment with both JNJ7777120 and naproxen alone. The coadministration of the two drugs was more effective. $^{**}P < 0.01$; $^{***}P < 0.001$ versus bleomycin + vehicle; $^{\circ\circ}P < 0.01$ versus bleomycin + JNJ7777120; $^{\#\#}P < 0.01$ versus bleomycin + naproxen. IB, immunoblotting; IP, immunoprecipitate.

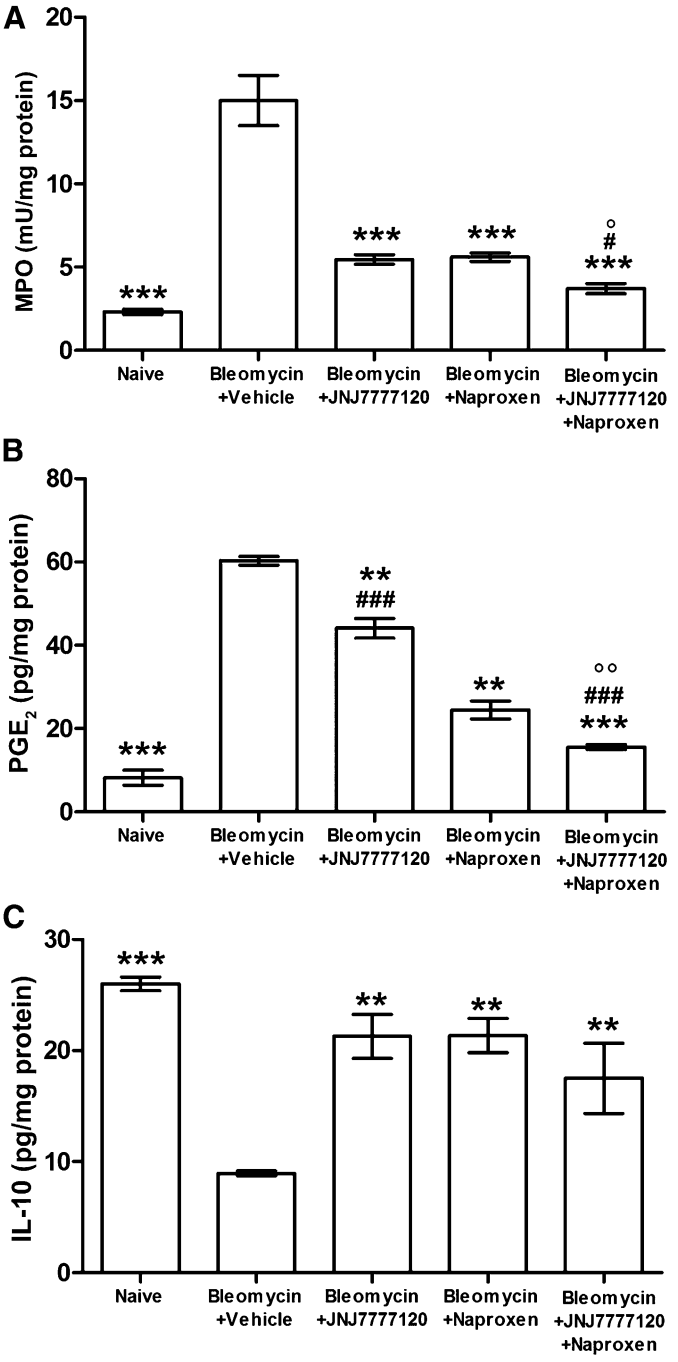

Fig. 6. Evaluation of inflammation parameters. (A) Bar graph showing the tissue levels (means ± S.E.M.) of the enzyme MPO, evaluated as the quantity of enzyme degrading 1 μmol of peroxide per minute at 37°C, from mice from the different experimental groups. (B) Bar graph showing the tissue levels of PGE_2 (means ± S.E.M.) for the different experimental groups. (C) Bar graph showing the tissue levels of the anti-inflammatory cytokine IL-10 (means ± S.E.M.) for the different experimental groups (one-way analysis of variance; n = 10 animals per group). $^{**}P < 0.01$; $^{***}P < 0.001$ versus bleomycin + vehicle; $^{\circ}P < 0.05$; $^{\circ\circ}P < 0.01$ versus bleomycin + JNJ7777120; $^{\#}P < 0.05$; $^{\#\#\#}P < 0.001$ versus bleomycin + naproxen.

the best characterized murine model in use today for lung fibrosis. Intratracheal delivery of bleomycin to rodents results in direct damage initially to alveolar epithelial cells, followed by the development of neutrophilic and lymphocytic panalveolitis within the first week and the development of fibrosis by day 14, with maximal responses generally around days 21–28 (Moore and Hogaboam, 2008). Chronic inflammatory conditions in the lungs lead to permanent structural changes and remodeling of the airway walls, whose fibrosis is a major constituent. Nowadays, there are no approved drugs that counteract the pathologic mechanism apart from some potential treatments targeting the TGF-β1 pathway, e.g., pirfenidone (Paz and Shoenfeld, 2010). Our experiments were performed in C57BL/6 mice, which are reported to be more susceptible to bleomycin-induced fibrosis than other strains, such as BALB/c mice (Schrier et al., 1983; Harrison and Lazo, 1987). Both drugs given alone or in combination were administered after the onset of bleomycin-induced lung injury by using a subcutaneously implanted micro-osmotic pump. This system allows sustained and long-term drug delivery, thus overcoming the pharmacokinetic limits of JNJ7777120, which has a maximal oral bioavailability of ~30% and a terminal half-life in mice of 1 hour (Thurmond et al., 2004).

In our experimental model, JNJ7777120, a selective receptor antagonist for H_4R, was compared with equimolar doses of naproxen. Compound JNJ7777120 has shown strong

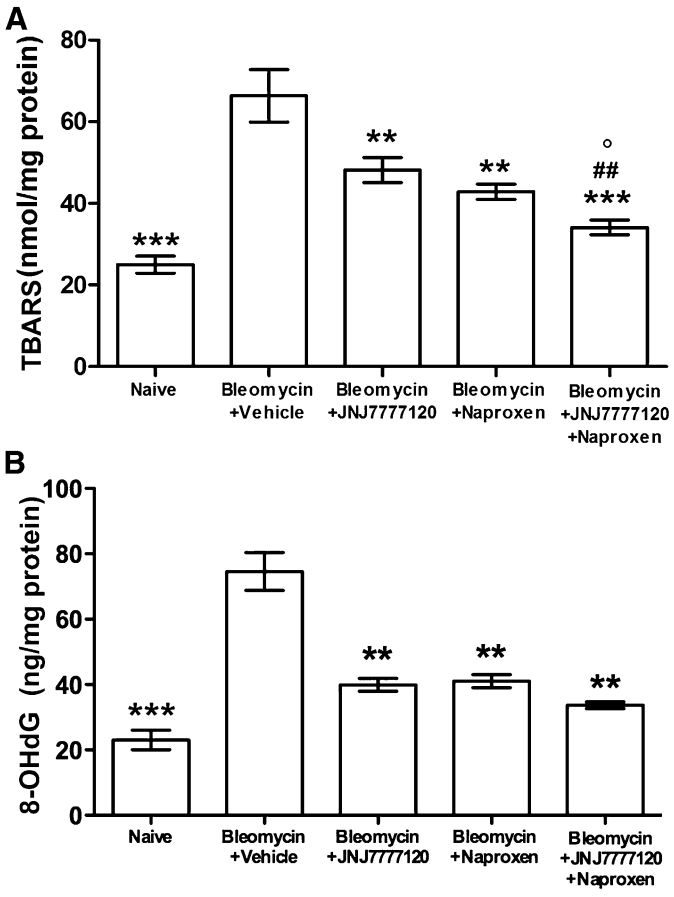

Fig. 7. Evaluation of oxidative stress parameters. (A) Bar graph showing the level of TBARS in lung tissue (means ± S.E.M.) in the different experimental groups. (B) Bar graph showing the levels of 8-OHdG (means ± S.E.M.) in the different experimental groups (one-way analysis of variance; $n = 10$ animals/group). $^{\circ}P < 0.05$ versus bleomycin + JNJ7777120; $^{\#\#}P < 0.01$ versus bleomycin + naproxen; $^{**}P < 0.01$; $^{***}P < 0.001$ versus bleomycin + vehicle.

anti-inflammatory properties, significantly decreasing histological and biochemical inflammatory parameters, such as the number of infiltrating leukocytes, and PGE_2 and IL-10 levels. When looking at the reduction of PGE_2 levels, which depends solely on cyclooxygenase (COX) inhibition, naproxen had a higher efficacy than JNJ7777120 ($P < 0.001$). On the other hand, when considering the other parameters, such as inhibition of leukocyte infiltration in the lung tissue and oxidative stress markers, JNJ7777120 was a little more effective than naproxen. When the two drugs were given together, we observed an additional effect conceivably determined by the complementary mechanisms acting on different proinflammatory targets. However, it can be speculated that the anti–TGF-β activity of JNJ7777120 may indirectly affect eicosanoid pathways by reducing TGF-β/Smad signaling, which is known to induce COX-2. Moreover, the hypothesis of a link between PGE_2 and TGF-β, already suggested (Alfranca et al., 2008), is herein supported; indeed, naproxen also downregulates TGF-β levels and Smad3/4 complex formation. COX-1 and COX-2 inhibitors, such as indomethacin, diclofenac, meloxicam, and naproxen, were reported to reduce lung collagen accumulation, inflammation, and oxidative stress in a bleomycin-induced lung fibrosis model (Thrall et al., 1979; Chandler and Young, 1989; Arafa et al., 2007; Pini et al., 2012), a model that highlights the inflammatory component of the pathology. Indeed, high levels of PGE_2 were reported in our positive fibrotic controls. However, evidence exists that PGE_2 has anti-inflammatory effects and inhibits collagen production (Saltzman et al., 1982), and that PGE_2 levels in patients with pulmonary fibrosis are significantly decreased, suggesting an ambiguous role of PGE_2 in lung fibroblast homeostasis. It is possible that prostaglandin inhibition can have a positive effect on the onset of lung fibrosis during the initial phase of inflammation and a detrimental effect during the fibrogenic events.

On the other side, the available data strongly support H_4R as a novel target for the pharmacologic modulation of immune and inflammatory disorders (Masini et al., 2013). Indeed, in inflammatory lung disorders, histamine acts as a mediator of both acute and chronic phases. H_4Rs are present at low levels in the lung, where their expression in bronchial epithelial and smooth muscle cells and microvascular endothelial cells (Gantner et al., 2002) can differently contribute to airway diseases. H_4R mediates redistribution and recruitment of mast cells in mucosal epithelium after allergen exposure (Thurmond et al., 2004); mediates the synergistic action of histamine and CXCL12, a chemokine involved in airway allergic disorders (Godot et al., 2007); and mediates the recruitment and response of regulatory T cells (Morgan et al., 2007).

The relevant effects of JNJ7777120 could be explained through the marked decrease in leukocyte infiltration in this in vivo model of pulmonary fibrosis, thus adding further evidence to the role of this receptor in controlling leukocyte trafficking and proinflammatory responses (Zampeli and Tiligada, 2009). These data suggest that JNJ7777120 may exert a favorable effect not only during the overt inflammatory phase of the disease, as previously reported with naproxen (Pini et al., 2012), but also during fibroblast proliferation. Indeed, previous data demonstrated a role for histamine and H_4R in fibroblast activation (Cowden et al., 2010), which is a pivotal event in the pathologic process related to disease progression (Garbuzenko et al., 2002; Kohyama et al., 2010). Here we report the effects of JNJ7777120 on the lung TGF-β pathway, collagen deposition, and goblet cell hyperplasia. In keeping with the demonstration that histamine modulates TGF-β/Smad signaling in conjunctival fibroblasts (Leonardi et al., 2011), our data confirm that the profibrotic effect of histamine is regulated by the activation of H_4R. Taken together, these results clearly indicate the antifibrotic effect of the H_4R antagonist.

On this background, our study suggests that the combination of the two drugs could be a promising therapeutic approach for pulmonary fibrosis. When naproxen and JNJ7777120 were coadministered, additive positive effects were measured on lung TGF-β signaling modulation, PGE_2, leukocytes, and goblet cell infiltration, confirming the effects of these drugs on the inflammatory phase. A single time point (24 days) was planned for this study. At this time point, a maximal fibrotic response was observed, and JNJ7777120 and naproxen, given in combination, exerted a maximal effect on most of the studied parameters.

Our data suggest that Smad3/4 complex formation plays a major role in determining the pharmacologic efficacy of the combination strategy herein proposed. Indeed, we propose that JNJ7777120, in reducing TGF-β and Smad3/4 complex formation, contributes to PGE_2 reduction, which is further

affected by naproxen, inhibiting COX-2. Therefore, by abolishing the PGE_2-mediated positive feedback on TGF-β/Smad signaling, this strategy becomes more effective than the use of each drug alone.

In conclusion, the results of the present study, supporting the hypothesis that H_4R antagonism exerts anti-inflammatory and antifibrotic effects in the model of bleomycin-induced lung fibrosis, indicate the therapeutic potential of the combination of H_4R antagonists and NSAIDs. Although JNJ7777120 itself is emerging as a promising therapeutic agent in lung inflammation and fibrosis, the combination with naproxen could have a distinct advantage over the single drug for the potentiating effect on the inhibition of inflammatory and profibrotic parameters. Moreover, this strategy could override the safety limitations of the existing anti-inflammatory drugs in the treatment of pulmonary fibrosis.

Authorship Contributions

Participated in research design: Rosa, Stark, Thurmond, Masini.

Conducted experiments: Rosa, Pini, Lucarini, Veglia, Lanzi.

Performed data analysis: Pini.

Wrote or contributed to the writing of the manuscript: Rosa, Veglia, Masini.

References

Alfranca A, López-Oliva JM, Genís L, López-Maderuelo D, Mirones I, Salvado D, Quesada AJ, Arroyo AG, and Redondo JM (2008) PGE2 induces angiogenesis via MT1-MMP-mediated activation of the TGFbeta/Alk5 signaling pathway. *Blood* **112**:1120–1128.

Arafa HM, Abdel-Wahab MH, El-Shafeey MF, Badary OA, and Hamada FM (2007) Anti-fibrotic effect of meloxicam in a murine lung fibrosis model. *Eur J Pharmacol* **564**:181–189.

Bai TR and Knight DA (2005) Structural changes in the airways in asthma: observations and consequences. *Clin Sci (Lond)* **108**:463–477.

Bradford MM (1976) A rapid and sensitive method for the quantitation of microgram quantities of protein utilizing the principle of protein-dye binding. *Anal Biochem* **72**:248–254.

Carter NJ (2011) Pirfenidone: in idiopathic pulmonary fibrosis. *Drugs* **71**:1721–1732.

Chandler DB and Young K (1989) The effect of diclofenac acid (Voltaren) on bleomycin-induced pulmonary fibrosis in hamsters. *Prostaglandins Leukot Essent Fatty Acids* **38**:9–14.

Chen HB, Rud JG, Lin K, and Xu L (2005) Nuclear targeting of transforming growth factor-beta-activated Smad complexes. *J Biol Chem* **280**:21329–21336.

Cowden JM, Riley JP, Ma JY, Thurmond RL, and Dunford PJ (2010) Histamine H4 receptor antagonism diminishes existing airway inflammation and dysfunction via modulation of Th2 cytokines. *Respir Res* **11**:86.

Davies HR, Richeldi L, and Walters EH (2003) Immunomodulatory agents for idiopathic pulmonary fibrosis. *Cochrane Database Syst Rev* (3):CD003134.

du Bois RM (2010) Strategies for treating idiopathic pulmonary fibrosis. *Nat Rev Drug Discov* **9**:129–140.

Gantner F, Sakai K, Tusche MW, Cruikshank WW, Center DM, and Bacon KB (2002) Histamine h(4) and h(2) receptors control histamine-induced interleukin-16 release from human CD8(+) T cells. *J Pharmacol Exp Ther* **303**:300–307.

Garbuzenko E, Nagler A, Pickholtz D, Gillery P, Reich R, Maquart FX, and Levi-Schaffer F (2002) Human mast cells stimulate fibroblast proliferation, collagen synthesis and lattice contraction: a direct role for mast cells in skin fibrosis. *Clin Exp Allergy* **32**:237–246.

Godot V, Arock M, Garcia G, Capel F, Flys C, Dy M, Emilie D, and Humbert M (2007) H4 histamine receptor mediates optimal migration of mast cell precursors to CXCL12. *J Allergy Clin Immunol* **120**:827–834.

Harrison JH, Jr and Lazo JS (1987) High dose continuous infusion of bleomycin in mice: a new model for drug-induced pulmonary fibrosis. *J Pharmacol Exp Ther* **243**:1185–1194.

Hauber HP and Blaukovitsch M (2010) Current and future treatment options in idiopathic pulmonary fibrosis. *Inflamm Allergy Drug Targets* **9**:158–172.

Kisseleva T and Brenner DA (2008) Fibrogenesis of parenchymal organs. *Proc Am Thorac Soc* **5**:338–342.

Kohyama T, Yamauchi Y, Takizawa H, Kamitani S, Kawasaki S, and Nagase T (2010) Histamine stimulates human lung fibroblast migration. *Mol Cell Biochem* **337**:77–81.

Leonardi A, Di Stefano A, Motterle L, Zavan B, Abatangelo G, and Brun P (2011) Transforming growth factor-β/Smad - signalling pathway and conjunctival remodelling in vernal keratoconjunctivitis. *Clin Exp Allergy* **41**:52–60.

Leonardi A, Radice M, Fregona IA, Plebani M, Abatangelo G, and Secchi AG (1999) Histamine effects on conjunctival fibroblasts from patients with vernal conjunctivitis. *Exp Eye Res* **68**:739–746.

Lodovici M, Casalini C, Cariaggi R, Michelucci L, and Dolara P (2000) Levels of 8-hydroxydeoxyguanosine as a marker of DNA damage in human leukocytes. *Free Radic Biol Med* **28**:13–17.

Masini E, Bani D, Vannacci A, Pierpaoli S, Mannaioni PF, Comhair SA, Xu W, Muscoli C, Erzurum SC, and Salvemini D (2005) Reduction of antigen-induced respiratory abnormalities and airway inflammation in sensitized guinea pigs by a superoxide dismutase mimetic. *Free Radic Biol Med* **39**:520–531.

Masini E, Lucarini L, Sydbom A, Dahlén B, and Dahlén S-E (2013) Histamine in asthmatic and fibrotic disorders, in *Histamine H4 Receptor: A Novel Drug Target* (Stark H ed) pp 145–171, Versita, London.

Moore BB and Hogaboam CM (2008) Murine models of pulmonary fibrosis. *Am J Physiol Lung Cell Mol Physiol* **294**:L152–L160.

Morgan RK, McAllister B, Cross L, Green DS, Kornfeld H, Center DM, and Cruikshank WW (2007) Histamine 4 receptor activation induces recruitment of FoxP3+ T cells and inhibits allergic asthma in a murine model. *J Immunol* **178**:8081–8089.

Mullane KM, Kraemer R, and Smith B (1985) Myeloperoxidase activity as a quantitative assessment of neutrophil infiltration into ischemic myocardium. *J Pharmacol Methods* **14**:157–167.

Ohkawa H, Ohishi N, and Yagi K (1979) Assay for lipid peroxides in animal tissues by thiobarbituric acid reaction. *Anal Biochem* **95**:351–358.

Paz Z and Shoenfeld Y (2010) Antifibrosis: to reverse the irreversible. *Clin Rev Allergy Immunol* **38**:276–286.

Pini A, Shemesh R, Samuel CS, Bathgate RA, Zauberman A, Hermesh C, Wool A, Bani D, and Rotman G (2010) Prevention of bleomycin-induced pulmonary fibrosis by a novel antifibrotic peptide with relaxin-like activity. *J Pharmacol Exp Ther* **335**:589–599.

Pini A, Viappiani S, Bolla M, Masini E, and Bani D (2012) Prevention of bleomycin-induced lung fibrosis in mice by a novel approach of parallel inhibition of cyclooxygenase and nitric-oxide donation using NCX 466, a prototype cyclooxygenase inhibitor and nitric-oxide donor. *J Pharmacol Exp Ther* **341**:493–499.

Raghu G, Collard HR, Egan JJ, Martinez FJ, Behr J, Brown KK, Colby TV, Cordier JF, Flaherty KR, and Lasky JA, et al.; ATS/ERS/JRS/ALAT Committee on Idiopathic Pulmonary Fibrosis (2011) An official ATS/ERS/JRS/ALAT statement: idiopathic pulmonary fibrosis: evidence-based guidelines for diagnosis and management. *Am J Respir Crit Care Med* **183**:788–824.

Richeldi L, Davies HR, Ferrara G, and Franco F (2003) Corticosteroids for idiopathic pulmonary fibrosis. *Cochrane Database Syst Rev* (3):CD002880.

Saltzman LE, Moss J, Berg RA, Hom B, and Crystal RG (1982) Modulation of collagen production by fibroblasts. Effects of chronic exposure to agonists that increase intracellular cyclic AMP. *Biochem J* **204**:25–30.

Sassoli C, Pini A, Chellini F, Mazzanti B, Nistri S, Nosi D, Saccardi R, Quercioli F, Zecchi-Orlandini S, and Formigli L (2012) Bone marrow mesenchymal stromal cells stimulate skeletal myoblast proliferation through the paracrine release of VEGF. *PLoS One* **7**:e37512.

Schrier DJ, Kunkel RG, and Phan SH (1983) The role of strain variation in murine bleomycin-induced pulmonary fibrosis. *Am Rev Respir Dis* **127**:63–66.

Sivakumar P, Ntolios P, Jenkins G, and Laurent G (2012) Into the matrix: targeting fibroblasts in pulmonary fibrosis. *Curr Opin Pulm Med* **18**:462–469.

Stramer BM, Mori R, and Martin P (2007) The inflammation-fibrosis link? A Jekyll and Hyde role for blood cells during wound repair. *J Invest Dermatol* **127**: 1009–1017.

Thrall RS, McCormick JR, Jack RM, McReynolds RA, and Ward PA (1979) Bleomycin-induced pulmonary fibrosis in the rat: inhibition by indomethacin. *Am J Pathol* **95**:117–130.

Thurmond RL, Desai PJ, Dunford PJ, Fung-Leung WP, Hofstra CL, Jiang W, Nguyen S, Riley JP, Sun S, and Williams KN, et al. (2004) A potent and selective histamine H4 receptor antagonist with anti-inflammatory properties. *J Pharmacol Exp Ther* **309**:404–413.

Wynn TA (2008) Cellular and molecular mechanisms of fibrosis. *J Pathol* **214**: 199–210.

Zampeli E and Tiligada E (2009) The role of histamine H4 receptor in immune and inflammatory disorders. *Br J Pharmacol* **157**:24–33.

Address correspondence to: Dr. Emanuela Masini, Department of NEUROFARBA, Section of Pharmacology, University of Florence, Viale G. Pieraccini n.6, 50139 Florence, Italy. E-mail: emanuela.masini@unifi.it